

**TEXAS UTILITIES GENERATING COMPANY**

SKYWAY TOWER • 100 NORTH OLIVE STREET, L.B. 81 • DALLAS, TEXAS 75201

May 16, 1984

Mr. B. J. Youngblood, Chief  
Licensing Branch No. 1  
U.S. Nuclear Regulatory Commission  
Washington, D.C. 20555

SUBJECT: COMANCHE PEAK STEAM ELECTRIC STATION  
DOCKET NOS. 50-445 and 50-446  
RESPONSE TO QUESTIONS ON HEATUP AND COOLDOWN  
CURVES FOR USE IN THE TECHNICAL SPECIFICATIONS

Dear Mr. Youngblood:

Enclosed are our responses to the questions transmitted to us by your letter dated December 9, 1983. It is requested that Figures 6 and 7 of the enclosure be included as Figures 3.4-2 and 3.4-3 of the Comanche Peak Technical Specifications.

If you have any questions about this matter please call Richard Werner at (214) 979-8227.

Respectfully submitted,

*J A Marshall* *for*

H. C. Schmidt

RAW:bjm  
Enclosure

9405220216 940516  
PDR ADCK 05000445  
A PDR

*Boo!*  
*1/1*

RESPONSE TO NRC QUESTIONS  
121.15 AND 121.16

FRACTURE AND NDE EVALUATIONS FOR  
THE CLOSURE FLANGE REGIONS OF  
COMANCHE PEAK UNITS 1 AND 2

# LIST OF ILLUSTRATIONS

FIGURE	TITLE	PAGE
1	CRITICAL CROSS SECTIONS	10
2	MECHANICAL BOUNDARY CONDITIONS	11
3	THERMAL BOUNDARY CONDITIONS	12
4	IMPACT OF NEW 10CFR50 RULE (WITHOUT ADDITIONAL STRESS ANALYSIS) ON COMANCHE PEAK UNITS 1 AND 2 REACTOR COOLANT SYSTEM HEATUP LIMITATIONS APPLICABLE UP TO 16 EFPY	13
5	IMPACT OF NEW 10CFR50 RULE (WITHOUT ADDITIONAL STRESS ANALYSIS) ON COMANCHE PEAK UNITS 1 AND 2 REACTOR COOLANT SYSTEM COOLDOWN LIMITATIONS APPLICABLE UP TO 16 EFPY	14
6	COMANCHE PEAK UNITS 1 AND 2 REACTOR COOLANT SYSTEM HEATUP LIMITATIONS APPLICABLE UP TO 16 EFPY	15
7	COMANCHE PEAK UNITS 1 AND 2 REACTOR COOLANT SYSTEM COOLDOWN LIMITATIONS APPLICABLE UP TO 16 EFPY	16
8	SHELL-TO-FLANGE WELD JOINT	17
9	HEAD-TO-FLANGE WELD JOINT	18

## TABLE OF CONTENTS

SECTION	TITLE	PAGE
1.0	INTRODUCTION	1
2.0	FINITE ELEMENT MODEL	2
2.1	Mechanical Boundary Conditions	3
2.2	Thermal Boundary Conditions	3
3.0	BOLTUP, PRESSURE AND THERMAL STRESSES	4
4.0	FRACTURE MECHANICS ANALYSIS	4
5.0	FRACTURE MECHANICS RESULTS	5
6.0	TECHNICAL SPECIFICATION PRESSURE-TEMPERATURE LIMIT	5
7.0	NDE METHODS	6
8.0	DETECTION AND SIZING ASSESSMENT	7

# LIST OF TABLES

TABLE	TITLE	PAGE
1	HEATUP TRANSIENT LONGITUDINAL STRESSES FOR CROSS SECTIONS 1, 2 AND 3	19
2	HEATUP TRANSIENT CIRCUMFERENTIAL STRESSES FOR CROSS SECTIONS 1, 2 AND 3	19
3	COOLDOWN TRANSIENT LONGITUDINAL STRESSES FOR CROSS SECTIONS 1, 2 AND 3	20
4	COOLDOWN TRANSIENT CIRCUMFERENTIAL STRESSES FOR CROSS SECTIONS 1, 2 AND 3	20
5	HEATUP TRANSIENT STRESS INTENSITY FACTORS ( $K_I$ ) FOR INSIDE SURFACE CIRCUMFERENTIAL FLAWS	21
6	HEATUP TRANSIENT STRESS INTENSITY FACTORS ( $K_I$ ) FOR OUTSIDE SURFACE CIRCUMFERENTIAL FLAWS	21
7	HEATUP TRANSIENT STRESS INTENSITY FACTORS ( $K_I$ ) FOR INSIDE SURFACE LONGITUDINAL FLAWS	22
8	HEATUP TRANSIENT STRESS INTENSITY FACTORS ( $K_I$ ) FOR OUTSIDE SURFACE LONGITUDINAL FLAWS	22
9	COOLDOWN TRANSIENT STRESS INTENSITY FACTORS ( $K_I$ ) FOR INSIDE SURFACE CIRCUMFERENTIAL FLAWS	23
10	COOLDOWN TRANSIENT STRESS INTENSITY FACTORS ( $K_I$ ) FOR OUTSIDE SURFACE CIRCUMFERENTIAL FLAWS	23
11	COOLDOWN TRANSIENT STRESS INTENSITY FACTORS ( $K_I$ ) FOR INSIDE SURFACE LONGITUDINAL FLAWS	24
12	COOLDOWN TRANSIENT STRESS INTENSITY FACTORS ( $K_I$ ) FOR OUTSIDE SURFACE LONGITUDINAL FLAWS	24

## 1.0 INTRODUCTION

This report provides the information requested by Reference 1 on the Westinghouse analysis which showed the closure flange regions of Comanche Peak Units 1 and 2 are less limiting than the beltline regions. As a result of this analysis, Westinghouse has shown that the Comanche Peak Units 1 and 2 heatup and cooldown curves are not impacted by the new 10CFR50<sup>[2]</sup> rule.

The new 10CFR50 rule states that when the pressure exceeds 20 percent of the preservice hydrostatic test pressure the temperature of the closure head and vessel flange regions must exceed the material  $RT_{NDT}$  by at least 120°F for normal operation and by 90°F for hydrostatic pressure tests and leak tests. For the Comanche Peak plants, 20 percent of the preservice hydrostatic test pressure is 621 psig. In addition, 10CFR50 states that exceptions to the new 10CFR50 rule can be made provided the NRC is in agreement with the analysis techniques used. As a result, Westinghouse has used a finite element model to show that the Comanche Peak closure flange regions do not actually impact the heatup and cooldown curves. Details of the analysis are given in this report. The specific information provided is listed as follows:

- 1) A description of the finite element analysis used to determine the stresses within the closure flange regions.
- 2) The bolt-up, pressure and thermal stresses determined by the finite element analysis at the inside and outside surface locations of the flange to head and flange to shell junctions.
- 3) How the bolt-up, pressure and thermal stresses were combined to determine the applied stress intensity factors.
- 4) The flaw geometry used to calculate the applied stress intensity factors.
- 5) The applied stress intensity factors for the flange to head and flange to shell junctions.

- 6) The Technical Specification pressure-temperature limit that will be used to pressurize the reactor vessel from 400 psig to leak test and hydrotest pressure prior to the leak test and hydrotest.
- 7) The non-destructive examination methods that are currently specified for inservice examinations of head flange-to-dome welds and flange-to-vessel welds.
- 8) A qualitative assessment of the flaw detection and sizing capabilities of the non-destructive examination methods described in Item 7.

## 2.0 FINITE ELEMENT MODEL

A two dimensional finite element model for a typical 4-loop reactor vessel closure head flange and vessel flange geometry was used in the analysis. The WECAN<sup>[3]</sup> finite element program was used to develop the model. The critical dimensions in this model are within 4 percent of the geometry for Comanche Peak Units 1 and 2. The finite element model was used to obtain temperature and stress gradients caused by the heatup and cool-down transients. Separate analyses were performed to determine the bolt-up, pressure, and thermal stresses. Figure 1 shows the cross sections analyzed.

Two-dimensional axisymmetric elements were used to model the closure flange regions of the reactor vessel. The bulk of the model is comprised of isotropic elements. constant strain elements were used for all the orthotropic elements as well as for any three node isotropic elements. Four node isoparametric elements were used for all the four node isotropic elements. Orthotropic elements were used to model the nuts, bolts, and the flange material between the bolt holes. These elements



were given a very low stiffness value in the hoop direction to account for the absence of any circumferential loads between adjacent members. The stainless steel clad, which covers the internal surfaces of the vessel, was considered to be non-structural and was not included as part of the finite element model. The insulating effect of the clad on model temperatures was included.

## 2.1 MECHANICAL BOUNDARY CONDITIONS

Physically, the reactor vessel shell will displace laterally, and the crown of the head does not displace laterally. To approximate this behavior, the bottom surface of the model in the shell region and the vertical surface of the model at the vessel crown were both assumed to be resting on rollers. This arrangement of restraint is assumed to correspond to the actual behavior of the vessel and prevents any rigid body motion of the model. Figure 2 shows this arrangement.

The initial bolt preload tensioning is designed to be so large that the mating flanges of the closure head and shell will never be separated by the contained coolant pressure. Because of this design, only bearing stresses can exist at the interface between the mating flanges of the head and shell. When the contained coolant pressure is zero, these bearing stresses exactly balance the bolt preload. As the coolant pressure increases, the flange bearing stresses diminish since the coolant pressure is now helping the flange bearing stresses in opposing the initial bolt preload.

## 2.2 THERMAL BOUNDARY CONDITIONS

For thermal analysis, all exterior surfaces of the model were assumed to be perfectly insulated and, therefore, adiabatic. Figure 3 shows the thermal boundary conditions. When the inside surface of the vessel is subjected to thermal transients, the primary mechanism of heat transfer is forced convection. The thermal properties of the metal are computed as linear functions of temperature. A uniform film coefficient was assumed for the entire inside surface of the vessel. Since the thermal resistance across the flange mating surfaces will not be significant, all the nodes on the flange mating surfaces were thermally coupled on the finite element model.



### 3.0 BOLTUP, PRESSURE AND THERMAL STRESSES

The boltup, pressure and thermal stresses for the heatup and cooldown transients are determined for the temperature range where the new 10CFR50 rule impacts the Comanche Peak Units 1 and 2 heatup and cooldown curves. The minimum temperature of the Comanche Peak closure flange regions is 160°F since the limiting  $RT_{NDT}$  is 40°F, and it occurs in the closure head flange region of both units. Figures 4 and 5 show that the 10CFR50 rule (without this special stress analysis) impacts the curves in the temperature range from 120°F to 160°F.

The thermal stresses used conservatively cover this temperature range for both the heatup and cooldown transients. For the heatup transient analysis, the thermal stresses near the middle of the 100°F/hour heatup transient are used. These stresses are obtained for a coolant temperature which is greater than the 120° to 160°F temperature range of interest. For the cooldown transient analysis, the thermal stresses at the end of 100°F/hour cooldown are used. These thermal stresses can be applied to the analysis which shows the new 10CFR50 rule does not impact the Comanche Peak heatup and cooldown curves.

The pressure stresses used in the analysis are based on an internal pressure of 776 psig since this is the maximum allowable pressure on Figures 4 and 5 in the temperature range from 120°F to 160°F.

Tables 1 through 4 contain the boltup, pressure, and thermal stresses for cross sections 1, 2, and 3. Table 1 contains the stresses in the longitudinal direction for the heatup transient, and Table 2 lists the heatup transient circumferential stresses. For the cooldown transient, Tables 3 and 4 contain the longitudinal and circumferential stresses, respectively.

### 4.0 FRACTURE MECHANICS ANALYSIS

The methods of the ASME Code Section XI, Appendix A<sup>[4]</sup> are used to generate the fracture analysis results. The flaw assumed in the analysis is a 0.625 inch deep surface flaw with an aspect ratio of 1:6. A safety factor of 2.0 is applied to the stress intensity factor due to the primary stresses (boltup and pressure stresses) as required by the ASME Code Section III, Appendix G<sup>[5]</sup>. Therefore, the primary and secondary (thermal) stress intensity

factors ( $K_I$ ) were combined in the following manner:

$$(K_I)_{\text{Total}} = 2 (K_I)_{\text{primary}} + (K_I)_{\text{secondary}} \quad (1)$$

In this report, the computed values of  $K_I$  which are negative are considered to be zero.

The NRC used the same fracture analysis techniques to develop the new 10CFR50 rule. The only difference is that Westinghouse used a finite element model to obtain stresses which are more accurate and less than the bending stress of 40 ksi conservatively assumed by the NRC.

## 5.0 FRACTURE MECHANICS RESULTS

The resultant primary, secondary, and total stress intensity factors for the heatup and cooldown transients are listed in Tables 5 through 12. For the heatup transient, Tables 5 and 6 contain the  $K_I$  values for inside and outside surface circumferential flaws, respectively. Tables 7 and 8 present the  $K_I$  values for inside and outside surface longitudinal flaws subjected to the heatup transient. For the cooldown transient, Tables 9 and 10 list the  $K_I$  values for inside and outside surface circumferential flaws, respectively. Tables 11 and 12 contain the  $K_I$  values for inside and outside surface longitudinal flaws subjected to the cooldown transient.

These results indicate that the maximum total  $K_I$  of  $64.74 \text{ ksi}\sqrt{\text{in}}$  occurs for an outside surface circumferential flaw at cross section 3 during cooldown (Table 10). This  $K_I$  is relatively small, and all the other  $K_I$  values in Tables 5 through 12 are smaller. Therefore, the Westinghouse analysis shows that the closure flange regions are less limiting than the Comanche Peak Units 1 and 2 heatup and cooldown curves in Figures 6 and 7.

## 6.0 TECHNICAL SPECIFICATION PRESSURE-TEMPERATURE LIMIT

This section describes the pressure-temperature limit that will be used to pressurize the reactor vessel from 400 psig to the leak test or hydrotest pressure. To reach the test pressure, follow the normal heatup curve in Figure 6 up to the minimum temperature required for the test. Then follow a vertical line (dashed in Figure 6) up to the desired test pressure.

## 7.0 NDE METHODS

Nondestructive examinations currently specified for inservice inspection of the reactor vessel flange-to-upper shell weld and the vessel head flange-to-dome weld are in accordance with Section XI of the ASME Boiler and Pressure Vessel Code [6]. Table IWB-2500-1 requires volumetric examination of flange-to-shell welds and volumetric and surface examinations of head flange-to-dome welds. The 1980 Edition of Section XI specifies the boundaries for volumetric examination include the weld and adjacent base material for a distance equal to one-half the weld thickness on both sides of the weld, Figures 8 and 9. The area specified for surface examination is the radiused or transition section of the flange on the outside surface as shown in Figure 9 between locations C and E.

Volumetric coverage of the reactor vessel flange-to-upper shell weld and specified adjacent base material is accomplished by two ultrasonic scan routines. Coverage from the flange side of the weld involves use of angled longitudinal waves from the flange seal surface. Beam angles are selected based on their ability to provide coverage of the weld and specified adjacent base material and provide near normal incidence to the plane of the weld. Refracted beam angles in the range  $0^{\circ}$  to  $16^{\circ}$  are typically used for these examinations. Examinations from the shell side of the weld involve  $0^{\circ}$ ,  $45^{\circ}$ , and  $60^{\circ}$  refracted angle beam coverage from the vessel inside diameter surface. Angle beam scanning is performed in two directions parallel to the weld and perpendicular to the weld from the shell side. Access for the shell side examinations is limited to outages when the core barrel is removed from the reactor vessel.

Volumetric examination of the reactor vessel closure head flange-to-dome weld and specified adjacent base material is accomplished by  $0^{\circ}$ ,  $45^{\circ}$  and  $60^{\circ}$  refracted angle coverage from the head outside surface. Angle beam scanning is performed in two directions parallel to the weld and perpendicular to the weld from the dome side. Surface examinations of the radiused or transition section of the head flange outside surface are conducted by a magnetic particle technique.

## 8.0 DETECTION AND SIZING ASSESSMENT

No quantitative information concerning detection and sizing capabilities of the techniques currently applied during examinations of closure flange junctions has been developed based upon qualification demonstrations, nor are such demonstrations specifically required by existing codes and standards. However, certain salient features of the examinations may be considered to establish that flaws of the type postulated in this analysis which fall within the volumes subject to examination are likely to be detected.

Flaws assumed for this analysis are 0.625 inch deep planar surface flaws with 1:6 aspect ratios. They may be oriented circumferentially or axially with respect to the vessel or head and may lie on the OD or ID surface.

The fact that the postulated flaws are surface related is significant from a detection probability point of view. Incipient cracks starting at right angles to a given surface (OD or ID) provide favorable conditions for detection via ASME Code specified 45° shear wave ultrasonic examinations from the opposite surface. Circumferential flaws are oriented favorably for detection during axial scanning. Axial flaws are oriented favorably for detection during circumferential scans. Circumferentially oriented flaws in the vessel flange weld region also provide favorable conditions for detection during ultrasonic examinations from the flange seal surface. Beam angles selected for these particular scans provide near normal incidence to the anticipated flaw plane thereby enhancing the probability of detection. Application of near surface examination methods in the form of full node 45° or shallow angle techniques significantly increases the probability of detecting flaws at the examination surface, i.e., the vessel inside and the head outside. Finally, the probability of detecting flaws which intersect the OD surface in areas of the vessel head subject to surface examination should be high.

While the qualitative assessment indicates that detection probabilities are reasonably good for flaws postulated in this analysis, certain unknown factors such as clad effects, defect roughness, orientation, and transparency due to

high compressive stresses influence the ability to detect and ultimately provide a realistic estimate of the size with current techniques. Defect sizing by ultrasonic methods has been the subject of several recent studies. To date, no single method has been identified which consistently provides precise sizing data. Typically several different methods must be applied and the most conservative results used in any analysis that might be necessary.

The state-of-the-art of reactor vessel examination has improved over the past several years. Enhanced near surface detection capabilities, trends toward lower recording levels, and tip-diffraction sizing methods are examples. Continued emphasis on NDE technique development promises to provide further improvements and more quantitative data concerning detection and sizing accuracies.



## 9.0 REFERENCES

1. Youngblood, B. J., "Heatup and Cooldown Curves for use in the Comanche Peak Technical Specifications", U.S. Nuclear Regulatory Commission, Washington, D.C., December 9, 1983.
2. Code of Federal Regulations, 10CFR50, Appendix G, "Fracture Toughness Requirements", U.S. Nuclear Regulatory Commission, Washington, D.C., Amended May 17, 1983 (48 Federal Register 24010).
3. WECAN Westinghouse Electric Computer Analysis User's Manual, Westinghouse R&D Center, Pittsburgh, Pennsylvania, September 17, 1979.
4. ASME Boiler and Pressure Vessel Code, Section XI, Division 1 - Appendix A, "Analysis of Flaw Indications", 1983 Edition.
5. ASME Boiler and Pressure Vessel Code, Section III, Division 1 - Appendix G, "Protection Against Nonductile Failure", 1983 Edition.
6. ASME Boiler and Pressure Vessel Code, Section XI, Division 1 - Subsection IWB, "Requirements for Class 1 Components of Light-Water Cooled Power Plants", 1980 Edition.

FIGURE 1  
CRITICAL CROSS SECTIONS

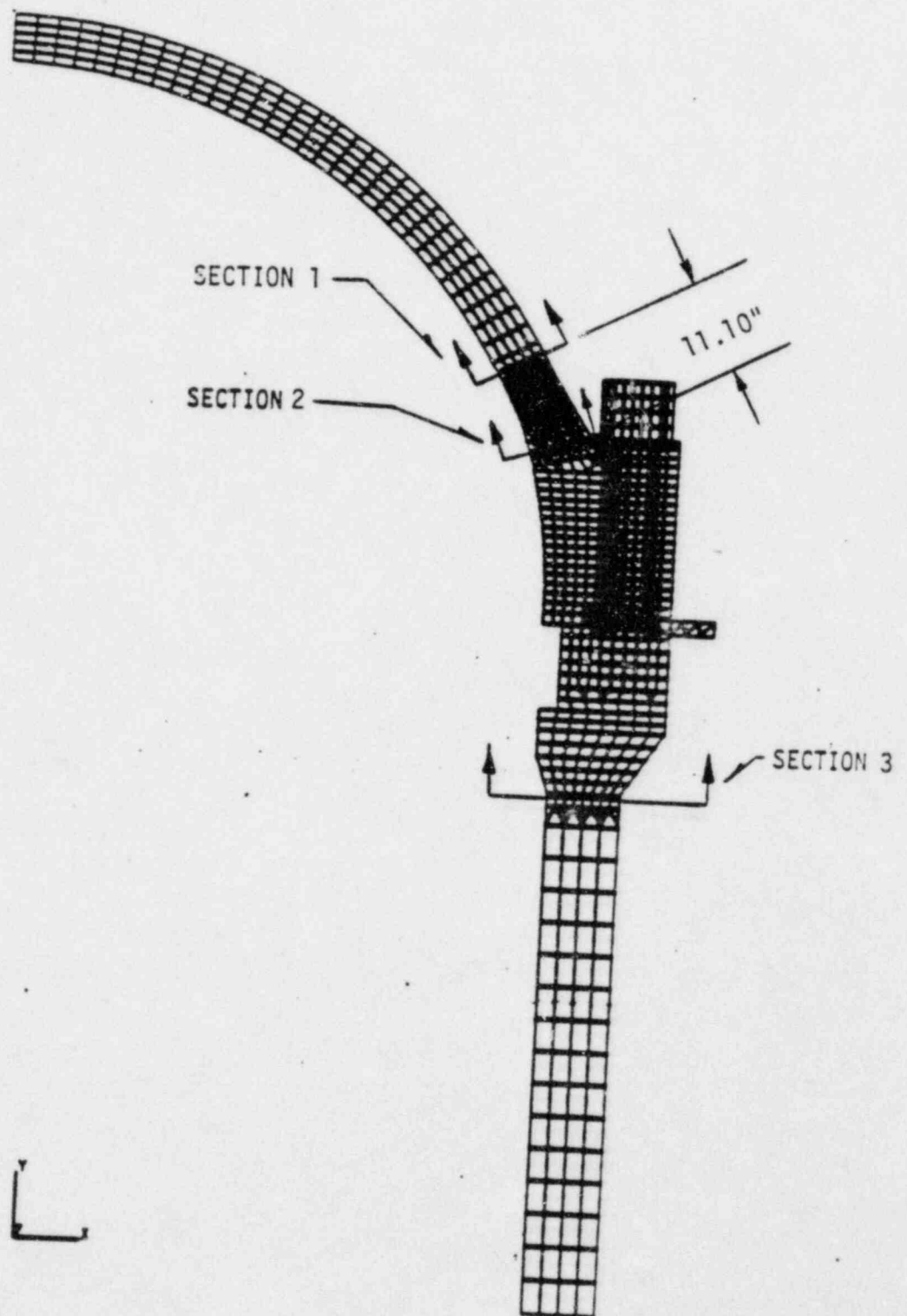




FIGURE 2  
MECHANICAL BOUNDARY CONDITIONS

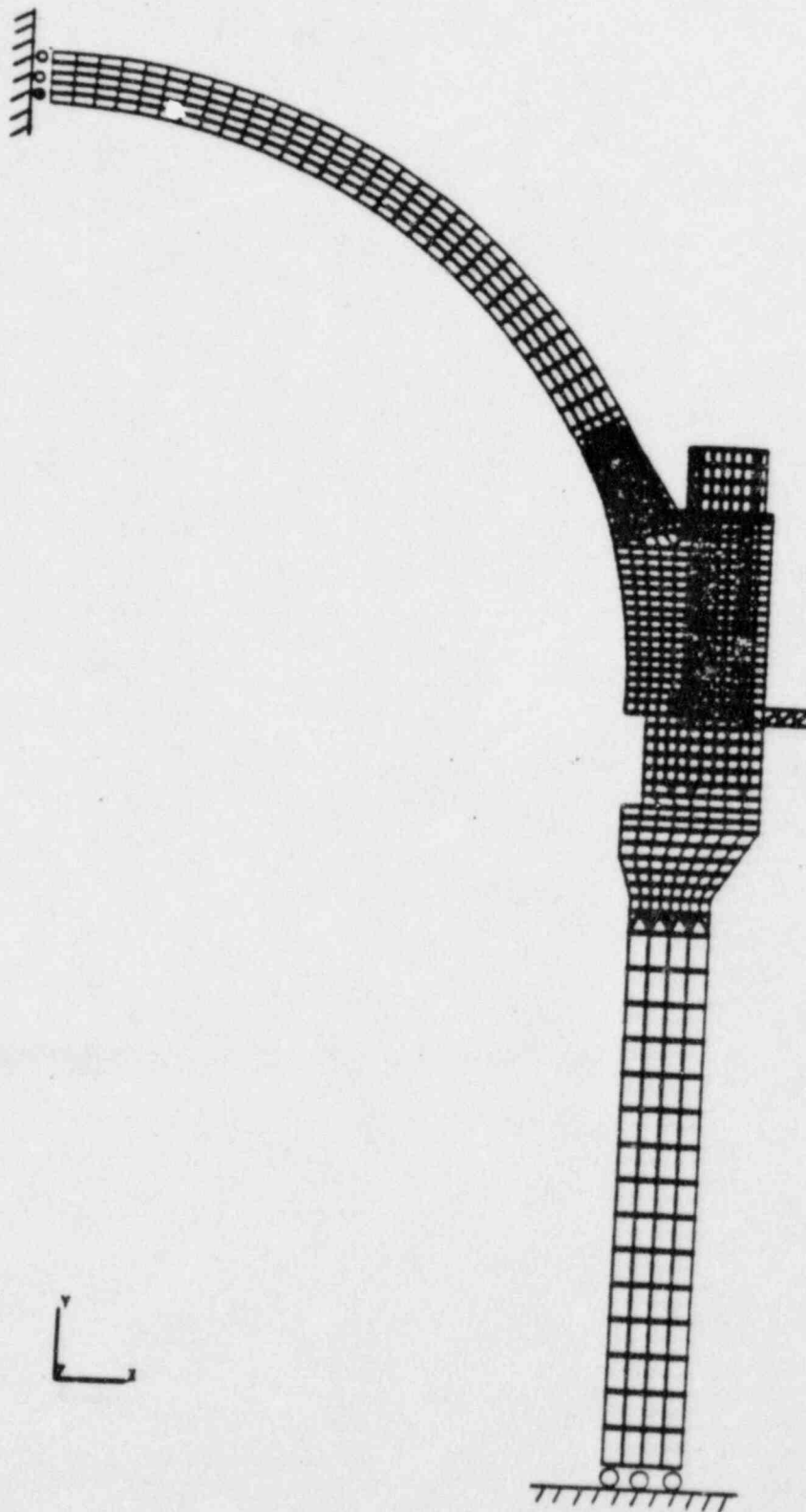
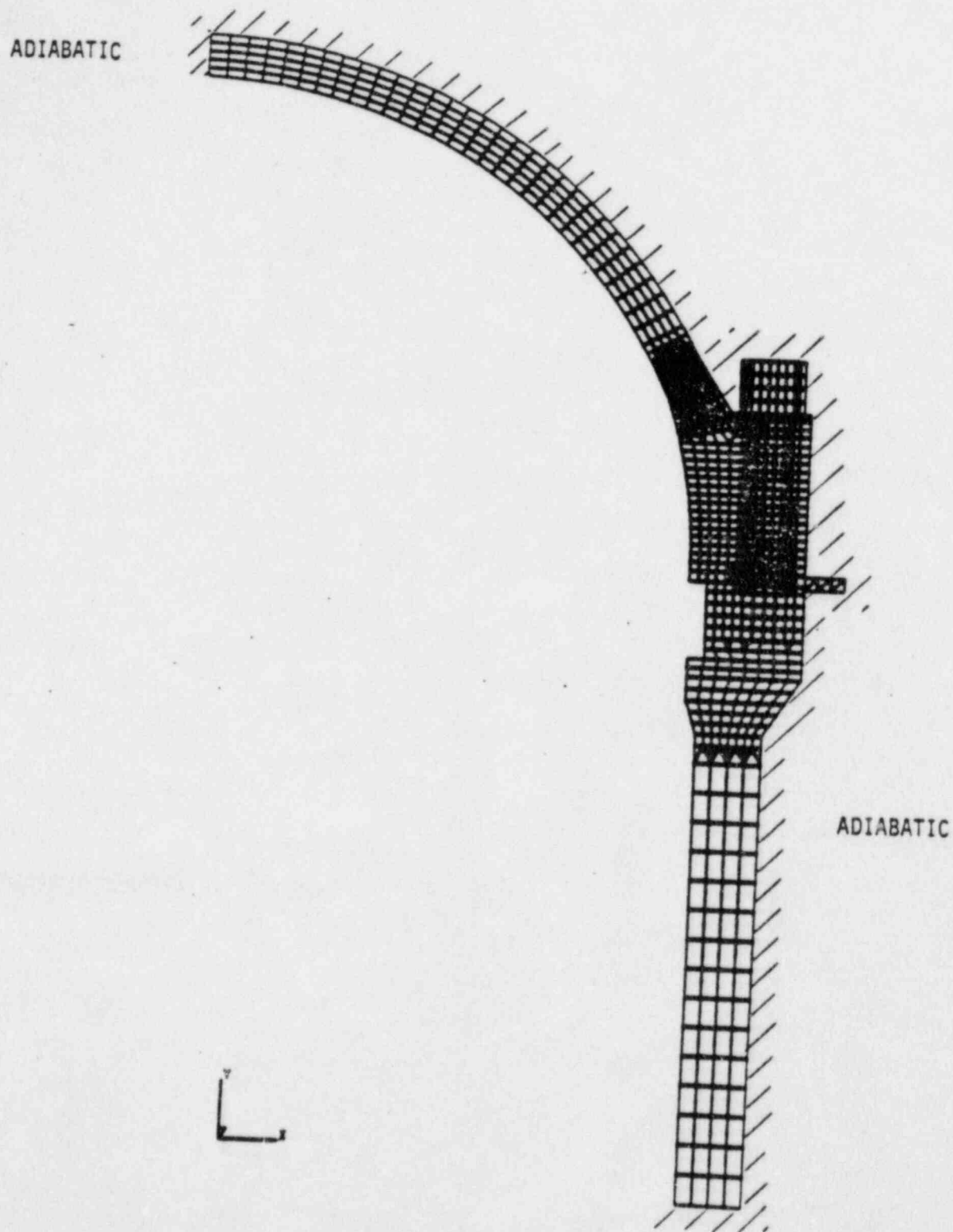


FIGURE 3  
THERMAL BOUNDARY CONDITIONS



MATERIAL PROPERTY BASIS

COPPER CONTENT : CONSERVATIVELY ASSUMED TO BE 0.10 WT%

RT<sub>NDT</sub> INITIAL : CONSERVATIVELY ASSUMED TO BE 40°F

RT<sub>NDT</sub> AFTER 16 EFPY : 1/4T, 110°F  
3/4T, 87°F

CURVE APPLICABLE FOR HEATUP RATES UP TO 60°F/HR FOR THE SERVICE PERIOD  
UP TO 16 EFPY AND CONTAINS MARGINS OF 10°F AND 60 PSIG FOR POSSIBLE  
INSTRUMENT ERRORS

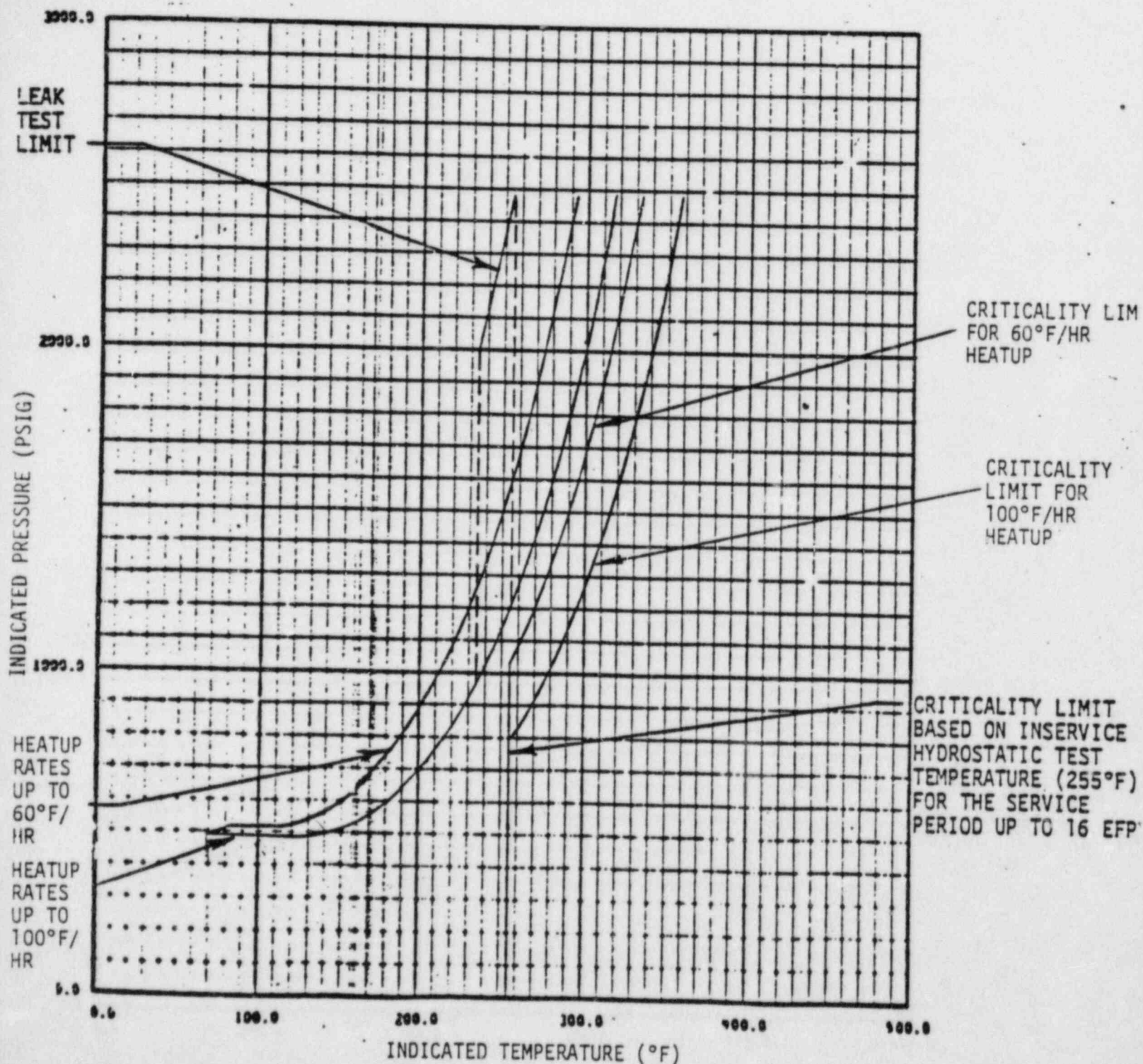


**Figure 4** IMPACT OF NEW 10CFR50 RULE (WITHOUT SPECIAL STRESS ANALYSIS) ON  
COMANCHE PEAK UNITS 1 AND 2 REACTOR COOLANT SYSTEM HEATUP LIMITA-  
TIONS APPLICABLE UP TO 16 EFPY

MATERIAL PROPERTY BASIS

COPPER CONTENT : CONSERVATIVELY ASSUMED TO BE 0.10 WT%

$RT_{NDT}$  INITIAL : CONSERVATIVELY ASSUMED TO BE 40°F

$RT_{NDT}$  AFTER 16 EFPY : 1/4T, 110°F  
3/4T, 87°F

CURVE APPLICABLE FOR COOLDOWN RATES UP TO 100°F/HR FOR THE SERVICE PERIOD UP TO 16 EFPY AND CONTAINS MARGINS OF 10°F AND 60 PSIG FOR POSSIBLE INSTRUMENT ERRORS

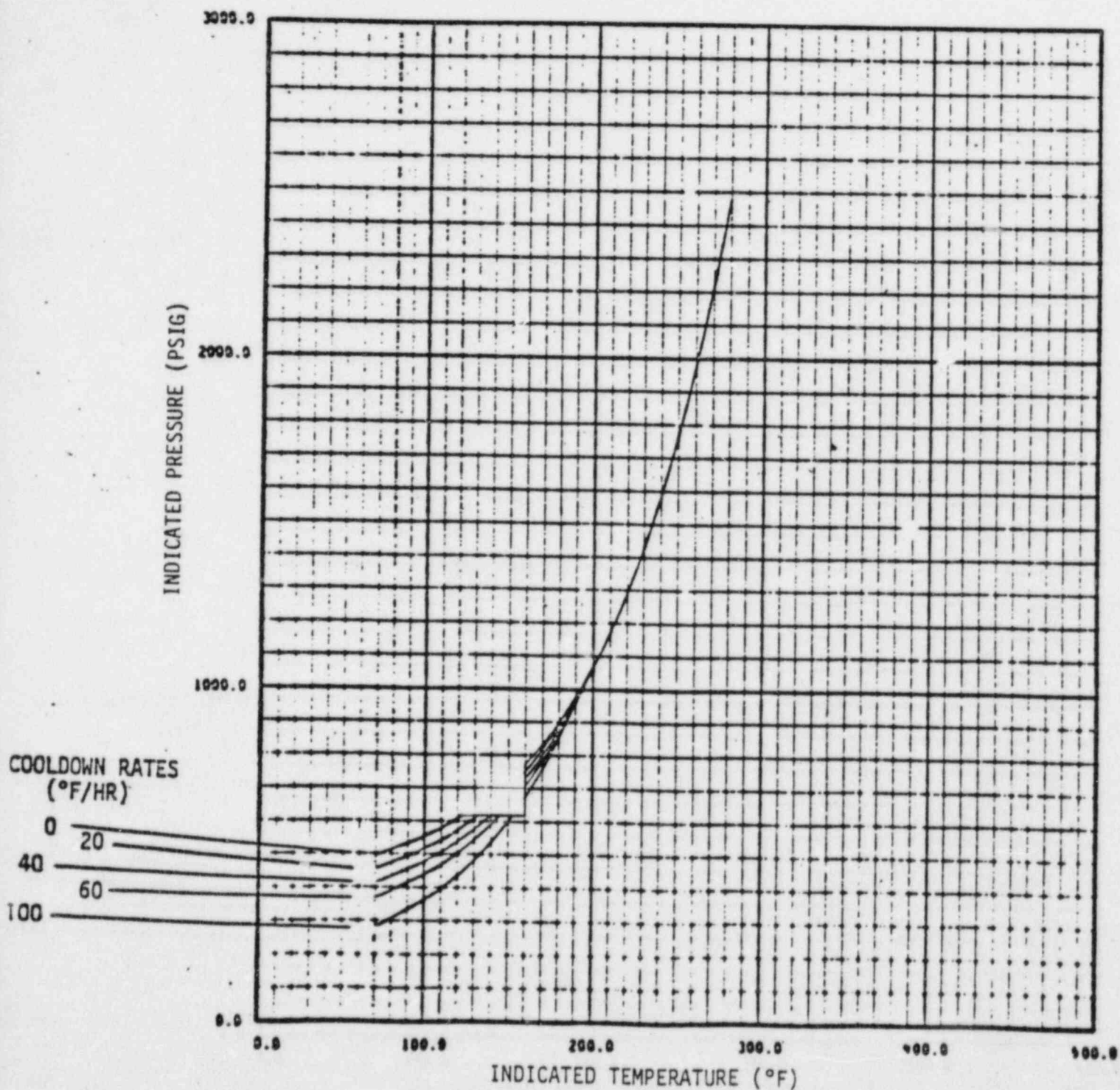


Figure 5 IMPACT OF NEW 10CFR50 RULE (WITHOUT SPECIAL STRESS ANALYSIS) ON COMANCHE PEAK UNITS 1 AND 2 REACTOR COOLANT SYSTEM COOLDOWN LIMITATIONS APPLICABLE UP TO 16 EFPY



MATERIAL PROPERTY BASIS

COPPER CONTENT : CONSERVATIVELY ASSUMED TO BE 0.10 WT%

RT<sub>NDT</sub> INITIAL : CONSERVATIVELY ASSUMED TO BE 40°F

RT<sub>NDT</sub> AFTER 16 EFPY : 1/4T, 110°F  
3/4T, 87°F

CURVE APPLICABLE FOR HEATUP RATES UP TO 60°F/HR FOR THE SERVICE PERIOD  
UP TO 16 EFPY AND CONTAINS MARGINS OF 10°F AND 60 PSIG FOR POSSIBLE  
INSTRUMENT ERRORS

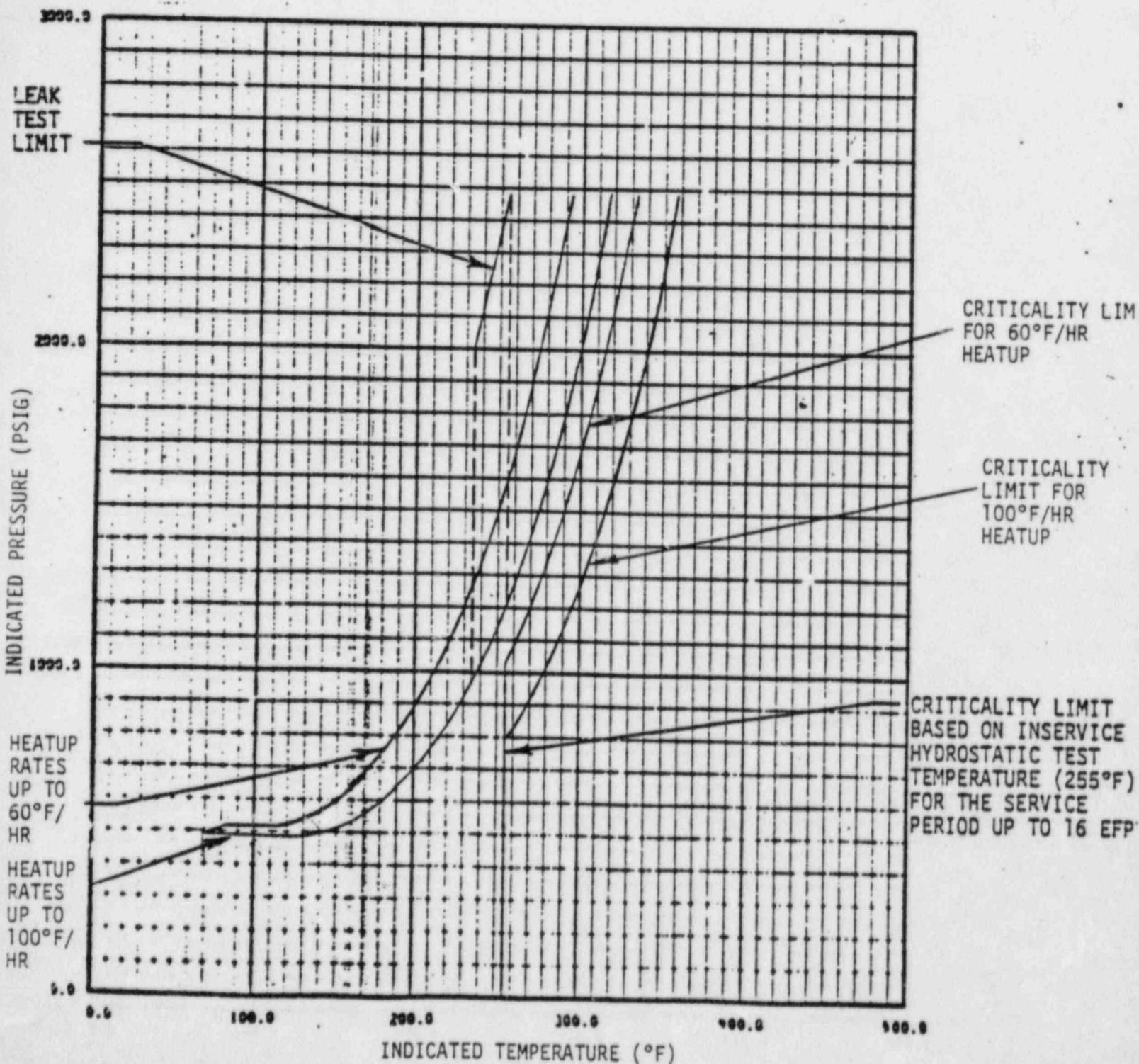


Figure 6 COMANCHE PEAK UNITS 1 AND 2 REACTOR COOLANT SYSTEM HEATUP LIMITATIONS APPLICABLE UP TO 16 EFPY

MATERIAL PROPERTY BASIS

COPPER CONTENT : CONSERVATIVELY ASSUMED TO BE 0.10 WT%

RT<sub>NDT</sub> INITIAL : CONSERVATIVELY ASSUMED TO BE 40°F

RT<sub>NDT</sub> AFTER 16 EFPY : 1/4T, 110°F  
3/4T, 87°F

CURVE APPLICABLE FOR COOLDOWN RATES UP TO 100°F/HR FOR THE SERVICE PERIOD UP TO 16 EFPY AND CONTAINS MARGINS OF 10°F AND 60 PSIG FOR POSSIBLE INSTRUMENT ERRORS

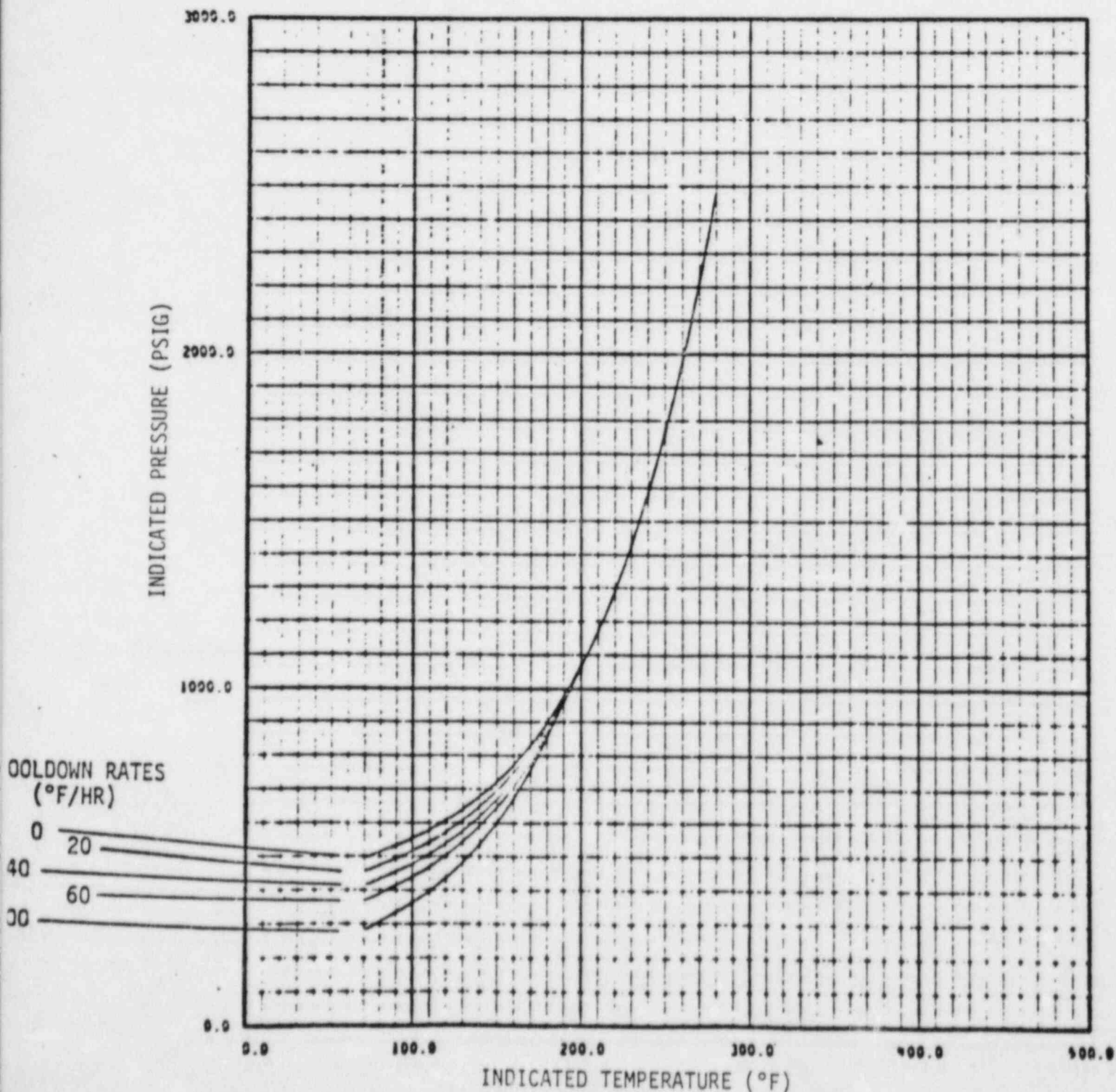


Figure 7 COMANCHE PEAK UNITS 1 AND 2 REACTOR COOLANT SYSTEM COOLDOWN LIMITATIONS APPLICABLE UP TO 16 EFPY





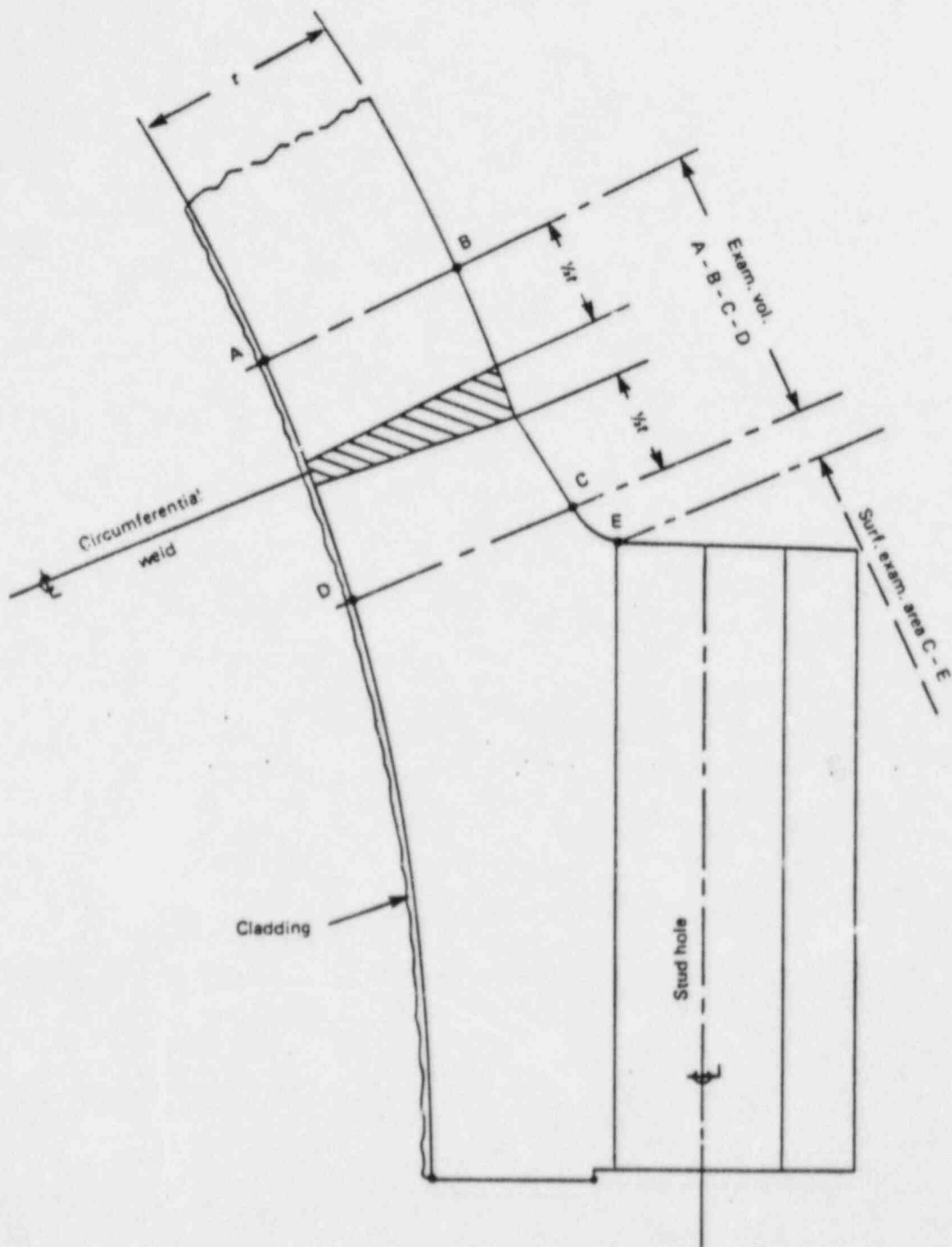


FIGURE 9: HEAD-TO-FLANGE WELD JOINT

TABLE 1

HEATUP TRANSIENT LONGITUDINAL STRESSES FOR CROSS SECTIONS 1, 2 AND 3

<u>Cross Section</u>	<u>Location</u>	<u>Boltup Stress (ksi)</u>	<u>Pressure Stress (ksi)</u>	<u>Thermal Stress (ksi)</u>	<u>Total Stress (ksi)</u>
1	Inside	-8.60	5.48	-12.32	-15.44
1	Outside	0.66	7.41	10.38	18.45
2	Inside	-10.78	4.71	-6.84	-12.91
2	Outside	8.37	2.70	3.34	14.41
3	Inside	-14.24	2.19	-8.96	-21.01
3	Outside	15.61	5.59	3.70	24.90

TABLE 2

HEATUP TRANSIENT CIRCUMFERENTIAL STRESSES FOR CROSS SECTIONS 1, 2 AND 3

<u>Cross Section</u>	<u>Location</u>	<u>Boltup Stress (ksi)</u>	<u>Pressure Stress (ksi)</u>	<u>Thermal Stress (ksi)</u>	<u>Total Stress (ksi)</u>
1	Inside	4.14	4.96	-14.57	-5.47
1	Outside	-5.33	5.29	5.91	5.87
2	Inside	3.74	4.39	-14.14	-6.01
2	Outside	-8.42	3.62	9.48	4.68
3	Inside	0.38	5.58	-15.89	-9.93
3	Outside	1.52	5.89	11.59	19.00

TABLE 3

COOLDOWN TRANSIENT LONGITUDINAL STRESSES FOR CROSS SECTIONS 1, 2 AND 3

<u>Cross Section</u>	<u>Location</u>	<u>Boltup Stress (ksi)</u>	<u>Pressure Stress (ksi)</u>	<u>Thermal Stress (ksi)</u>	<u>Total Stress (ksi)</u>
1	Inside	-8.60	5.48	17.65	14.53
1	Outside	0.66	7.41	-15.66	-7.59
2	Inside	-10.78	4.71	11.13	5.06
2	Outside	8.37	2.70	-3.37	7.70
3	Inside	-14.24	2.19	20.26	8.21
3	Outside	15.61	5.59	-7.79	13.41

TABLE 4

COOLDOWN TRANSIENT CIRCUMFERENTIAL STRESSES FOR CROSS SECTIONS 1, 2 AND 3

<u>Cross Section</u>	<u>Location</u>	<u>Boltup Stress (ksi)</u>	<u>Pressure Stress (ksi)</u>	<u>Thermal Stress (ksi)</u>	<u>Total Stress (ksi)</u>
1	Inside	4.14	4.96	19.98	29.08
1	Outside	-5.33	5.29	-4.11	-4.15
2	Inside	3.74	4.39	23.40	31.53
2	Outside	-8.42	3.62	-2.61	-7.41
3	Inside	0.38	5.58	25.34	31.30
3	Outside	1.52	5.89	-10.13	-2.72

TABLE 5

HEATUP TRANSIENT STRESS INTENSITY FACTORS ( $K_I$ ) FOR  
INSIDE SURFACE CIRCUMFERENTIAL FLAWS<sup>1</sup>

<u>CROSS SECTION</u>	<u>PRIMARY <math>K_I</math> (ksi<math>\sqrt{in}</math>)<sup>I</sup></u>	<u>SECONDARY <math>K_I</math> (ksi<math>\sqrt{in}</math>)<sup>I</sup></u>	<u>TOTAL <math>K_I</math> (ksi<math>\sqrt{in}</math>)<sup>I</sup></u>
1	3.51	0.00	7.02
2	3.48	0.00	6.96
3	6.48	0.00	12.96

TABLE 6

HEATUP TRANSIENT STRESS INTENSITY FACTORS ( $K_I$ ) FOR  
OUTSIDE SURFACE CIRCUMFERENTIAL FLAWS<sup>1</sup>

<u>CROSS SECTION</u>	<u>PRIMARY <math>K_I</math> (ksi<math>\sqrt{in}</math>)<sup>I</sup></u>	<u>SECONDARY <math>K_I</math> (ksi<math>\sqrt{in}</math>)<sup>I</sup></u>	<u>TOTAL <math>K_I</math> (ksi<math>\sqrt{in}</math>)<sup>I</sup></u>
1	10.43	14.04	34.90
2	14.16	6.34	34.66
3	27.95	8.17	64.07

TABLE 7

HEATUP TRANSIENT STRESS INTENSITY FACTORS ( $K_I$ ) FOR  
INSIDE SURFACE LONGITUDINAL FLAWS

<u>CROSS SECTION</u>	<u>PRIMARY <math>K_I</math> (ksi<math>\sqrt{in}</math>)</u>	<u>SECONDARY <math>K_I</math> (ksi<math>\sqrt{in}</math>)</u>	<u>TOTAL <math>K_I</math> (ksi<math>\sqrt{in}</math>)</u>
1	12.26	0.00	24.52
2	10.63	0.00	21.26
3	9.58	0.00	19.16

TABLE 8

HEATUP TRANSIENT STRESS INTENSITY FACTORS ( $K_I$ ) FOR  
OUTSIDE SURFACE LONGITUDINAL FLAWS

<u>CROSS SECTION</u>	<u>PRIMARY <math>K_I</math> (ksi<math>\sqrt{in}</math>)</u>	<u>SECONDARY <math>K_I</math> (ksi<math>\sqrt{in}</math>)</u>	<u>TOTAL <math>K_I</math> (ksi<math>\sqrt{in}</math>)</u>
1	6.37	12.59	25.33
2	2.31	14.65	19.27
3	10.33	17.55	38.21

TABLE 9

COOLDOWN TRANSIENT STRESS INTENSITY FACTORS ( $K_I$ ) FOR  
INSIDE SURFACE CIRCUMFERENTIAL FLAWS

<u>CROSS SECTION</u>	<u>PRIMARY <math>K_I</math> (ksi<math>\sqrt{in}</math>)</u>	<u>SECONDARY <math>K_I</math> (ksi<math>\sqrt{in}</math>)</u>	<u>TOTAL <math>K_I</math> (ksi<math>\sqrt{in}</math>)</u>
1	3.51	22.02	29.04
2	3.48	14.40	21.36
3	6.48	26.83	39.79

TABLE 10

COOLDOWN TRANSIENT STRESS INTENSITY FACTORS ( $K_I$ ) FOR  
OUTSIDE SURFACE CIRCUMFERENTIAL FLAWS

<u>CROSS SECTION</u>	<u>PRIMARY <math>K_I</math> (ksi<math>\sqrt{in}</math>)</u>	<u>SECONDARY <math>K_I</math> (ksi<math>\sqrt{in}</math>)</u>	<u>TOTAL <math>K_I</math> (ksi<math>\sqrt{in}</math>)</u>
1	10.43	1.40	22.26
2	14.16	5.41	33.73
3	27.95	8.84	64.74

TABLE 11

COOLDOWN TRANSIENT STRESS INTENSITY FACTORS ( $K_I$ ) FOR  
INSIDE SURFACE LONGITUDINAL FLAWS

<u>CROSS SECTION</u>	<u>PRIMARY <math>K_I</math> (ksi<math>\sqrt{in}</math>)</u>	<u>SECONDARY <math>K_I</math> (ksi<math>\sqrt{in}</math>)</u>	<u>TOTAL <math>K_I</math> (ksi<math>\sqrt{in}</math>)</u>
1	12.26	26.56	51.08
2	10.63	31.53	52.79
3	9.58	34.04	53.20

TABLE 12

COOLDOWN TRANSIENT STRESS INTENSITY FACTORS ( $K_I$ ) FOR  
OUTSIDE SURFACE LONGITUDINAL FLAWS

<u>CROSS SECTION</u>	<u>PRIMARY <math>K_I</math> (ksi<math>\sqrt{in}</math>)</u>	<u>SECONDARY <math>K_I</math> (ksi<math>\sqrt{in}</math>)</u>	<u>TOTAL <math>K_I</math> (ksi<math>\sqrt{in}</math>)</u>
1	6.37	11.15	23.89
2	2.31	14.47	19.09
3	10.33	10.60	31.26